Available online at www.sciencedirect.com
ScienceDirect
Geochimica et Cosmochimica Acta 73 (2009) 3948–3962
Geochimica et Cosmochimica Acta
www.elsevier.com/locate/gca

Mass-independent fractionation of oxygen isotopes in the mesostasis of a chondrule from the Semarkona LL3.0 ordinary chondrite

Derek W.G. Sears [a,*], John M. Saxton [a,c], Ian C. Lyon [b]

[a] Arkansas Center for Space and Planetary Sciences and Department of Chemistry and Biochemistry, University of Arkansas, Fayetteville, AR 72701, USA
[b] School of Earth, Atmospheric and Environmental Sciences, University of Manchester, Manchester M13 9PL, UK
[c] Nu Instruments Ltd., 74 Clywedog Rd. South, Wrexham LL13 9XS, UK

Received 28 June 2007; accepted in revised form 2 April 2009; available online 9 April 2009

Abstract

A large chondrule from Semarkona, the most primitive ordinary chondrite known, has been discovered to contain a record of mass transport during its formation. In most respects, it is a normal Type I, group A1, low-FeO chondrule that was produced by reduction and mass-loss during the unidentified flash-heating event that produced the chondrules, the most abundant structural component in primitive meteorites. We have previously measured elemental abundances and abundance profiles in this chondrule. We here report oxygen isotope ratio abundances and ratio abundance profiles. We have found that the mesostasis is zoned in oxygen isotope ratio, with the center of the chondrule containing isotopically heavier oxygen than the outer regions, the outer regions being volatile rich from the diffusion of volatiles into the chondrule during cooling. The $\delta^{17}O$ values range from $-2.0‰$ to $9.9‰$, while $\delta^{18}O$ range from $-1.9‰$ to $9.6‰$. More importantly, a plot of $\delta^{17}O$ against $\delta^{18}O$ has a slope of 1.1 ± 0.2 (1σ) and 0.88 ± 0.10 (1σ) when measured by two independent methods. Co-variation of $\delta^{17}O$ with $\delta^{18}O$ that does not follow mass-dependent fractionation has often been seen in primitive solar system materials and is usually ascribed to the mixing of different oxygen reservoirs. We argue that petrographic and compositional data indicate that this chondrule was completely melted at the time of its formation so that relic grains could not have survived. Furthermore, there is petrographic and compositional evidence that there was no aqueous alteration of this chondrule subsequent to its formation. Although it is possible to formulate a series of exchanges between the chondrule and external ^{16}O-rich and ^{16}O-poor reservoirs that may explain the detailed oxygen isotope systematics of this chondrule, such a sequence of events looks very contrived. We therefore hypothesize that reduction, devolatilization, and crystallization of the chondrule melt may have produced ^{16}O-rich olivines and ^{16}O-poor mesostasis plotting on a slope-one line as part of the chondrule-forming process in an analogous fashion to known chemical mass-independent isotopic fractionation mechanisms. During cooling, volatiles and oxygen near the terrestrial line in oxygen isotope composition produced the outer zone of volatile rich and ^{16}O-rich mesostasis. The chondrule therefore not only retains a record of considerable mass transport accompanying formation, but also may indicate that the isotopes of oxygen underwent mass-independent fractionation during the process.

1. INTRODUCTION

The chondritic meteorites are remnants from the earliest phases of solar system history. A relatively small number appear to have suffered only minimal alteration since agglomeration, and these have the potential to provide unique insights into their formation and early history (Sears, 2004; Lauretta and McSween, 2006; Scott, 2007). The chondrules, glassy submillimeter spherules, comprise a major component of most chondritic meteorites (Sears, 2004, and references therein). They reach ~75% by volume of

* Corresponding author. Fax: +1 479 575 7778.

0016-7037/$ - see front matter © 2009 Elsevier Ltd. All rights reserved.
doi:10.1016/j.gca.2009.04.002

the ordinary chondrites, the most common class of meteorites. Although it has long been known that chondrules are completely or partially melted silicate droplets (Sorby, 1864), details of their origin remain elusive two-hundred years after their discovery (Howard, 1802; Boss, 1996). Clearly they are crucial to understanding the origin and history of early solar system matter. In as much as the abundance and properties of chondrules varies from chondrite class to chondrite class, their formation probably also has relevance to the formation of the classes and the distinctive properties of each (Sears, 2004).

One of the most important characteristics of primitive solar system materials is their oxygen isotope properties, not just the proportions of the three isotopes of oxygen (^{16}O, ^{17}O and ^{18}O) but also their co-variation (Clayton, 2008). When meteorite data are plotted as $\delta^{17}O$ against $\delta^{18}O$, where

$$\delta^{17,18}O = 1000 \times \{(^{17,18}O/^{16}O)_{sample}/(^{17,18}O/^{16}O)_{standard}) - 1\},$$

each of the major classes plots in a unique field or along a unique correlation line. Lunar and terrestrial samples (with only rare exceptions), plot on a line with slope ~0.52, consistent with mass-dependent fractionation. (Isotopic ratio analyses achievable by ion probe are typically accurate to ~1‰ so that mass fractionation lines discussed here are therefore only given to two decimal places.) Mass-dependent fractionation of isotopes is a characteristic of common chemical and physical processes such as evaporation, condensation, crystallization, etc. However, many mineral components from the ordinary chondrites, chondrules from ordinary chondrites. and anhydrous mineral phases from carbonaceous chondrites plot on lines with slopes close to unity requiring mass-independent fractionation of O isotopes (Clayton and Mayeda, 1984, 1999; Macpherson et al., 1988; Clayton et al., 1991; Young and Russell, 1998; Kobayashi et al., 2003; Krot et al., 2006; Sakamoto et al., 2007).

The slope-one lines are often assumed to be mixing lines between two components. An early explanation for a ^{16}O-enriched reservoir was the heterogeneous mixing of nucleosynthetically generated ^{16}O injected into the early solar nebula with an ^{16}O-poor component (Clayton et al., 1973). However, the lack of similar wide-spread excesses of ^{24}Mg and ^{28}Si in meteoritic material, and the finding that presolar oxide grains were rare and tended to be more enriched in ^{17}O than ^{16}O, make this idea unappealing (Nittler, 2003).

Mechanisms that produce mass-independent fractionations from a single homogeneous component have been postulated. One such mechanism is photochemical self-shielding in the early solar nebula or parent molecular cloud. For example, the CO molecule absorbs ultraviolet light at specific wavelengths that depend on the isotope of oxygen present. The incident radiation breaks the molecular bond. Because ^{16}O is 500 times more abundant than ^{18}O and 2500 times more abundant the ^{17}O, the surface region of a molecular cloud or the solar nebula will become optically thick to the radiation that breaks $C^{16}O$, but the radiation that will break $C^{17}O$ and $C^{18}O$ will continue deeper into the cloud, producing a region when only ^{17}O and ^{18}O are free to react and form other compounds (e.g., H_2O). The result is that the cloud is heterogeneous in the ionization of CO isotopologues (molecules of the same chemistry but different in their isotopic composition) with $C^{16}O$ remaining neutral deeper in the cloud and available for reactions whereas $C^{17}O$ and $C^{18}O$ are ionized and dissociated. This mechanism was first proposed by Thiemens and Heidenreich (1983) and re-proposed and developed by Clayton (2002). There were difficulties with this model in that unless density conditions were favorable, competing chemical reactions would rapidly homogenize mass-independent fractionation effects.

It might be that the isotopic shifts are preserved by the formation of water, which can easily be separated from CO by physical means, but then there are issues in transferring these isotopic signatures from their formation locations to the solid phases in the inner solar system (Lunine et al., 2007). Ways around this were proposed by considering photoionization of CO above the plane of the protosolar accretion disc (Young and Lyons, 2003; Lyons and Young, 2005; Young, 2007) or moving the self-shielding photochemical mechanisms to the progenitor molecular cloud (Yurimoto and Kuramoto, 2004). The self-shielding mechanism is appealing in that it has been observed to cause variable enhancements of the CO isotopomers in molecular clouds but the details of the mechanism and its possible applicability to the observation of mass-independent fractionation of oxygen isotopes in the early solar system is still vigorously debated (Krot et al., 2006; Ali and Nuth, 2007; Gounelle and Meibom, 2007; Chakraborty et al., 2008; Clayton, 2008; Davis et al., 2008; Lyons et al., 2008; Young et al., 2008; Yurimoto et al., 2008).

An alternative possibility is that the mass-independent fractionation occurred as the result of symmetry-selective chemistry or photochemical effects similar to processes that occur in the upper atmosphere and which can be reproduced in the laboratory (Thiemens, 1996, 1999, 2006; Chakraborty and Bhattacharya, 2003; Romero and Thiemens, 2003; Savarino et al., 2003; Ali and Nuth, 2007; Kimura et al., 2007). This isotopic fractionation mechanism relies upon symmetry in molecules or density of quantum states being different for different isotopologues. Rates of reaction for symmetric molecules such as $^{16}O^{16}O^{16}O$ are different from that for $^{17}O^{16}O^{16}O$ or $^{18}O^{16}O^{16}O$ and this provides the mechanism for mass-independent fractionation. Although much of the early research done upon such systems concentrated upon ozone and gas phase reactions, it has recently been shown that the chemical mass-independent fractionation effect can occur in a range of molecules and for reactions on solid surfaces (Marcus, 2004; Thiemens, 2006; Ali and Nuth, 2007; Kimura et al., 2007) and that (apart from water vapor), the oxygen in most atmospheric gases are fractionated mass-independently (Thiemens, 2006). Young et al. (2008) state that the chemical mass-independent fractionation effect is attractive because of its simplicity but were unclear as to how the isotopic signature of the gas could be trapped in the solid and there is a lack of experimental evidence that such mechanisms can have significantly contributed to forming wide-spread mass-independent fractionation of oxygen isotopes in the early solar system.

A significant difference between these models are the predictions that if the wide-spread mass-independent oxygen isotope fractionation in the early solar system resulted from a self-shielding mechanism then it may be expected that the oxygen isotope composition of the sun would be significantly ^{16}O enriched compared to the remaining solar system materials. If more local chemical mass-independent fractionation mechanisms produced the observed ^{16}O enrichments of early solar system materials then it is likely that the average oxygen isotope composition of the sun would be very similar to the average of early solar system solids (which spread widely but center on $\delta^{18}O$ and $\delta^{17}O$ of ~0‰, ~0‰ (V-SMOW)). Preliminary measurements of δ18O and $\delta^{17}O$ of ~−70‰, −70‰, respectively, for the oxygen isotopic composition of the sun (Hand, 2008; McKeegan et al., 2008), clearly favor the self-shielding model, although there are many potential elemental and isotopic alteration processes between the initial solar gaseous nebula and the solid components in meteorites.

Several authors have explored the exchange of oxygen between chondrules and the ambient gas by looking for correlations between oxygen isotopes and chondrule size (Bridges et al., 1998, 1999). However, the work is very difficult and until recently, chondrules were generally too small to analyze individually by techniques other than ion probes, so large numbers of chondrules of different histories were combined. Sometimes meteorites of high petrographic type were analyzed, so primary properties were confused with a metamorphic overprint. Even when analyzed individually, the multi-minerallic nature of chondrules was a problem as oxygen isotope properties then reflect mineral proportions. It was also difficult-to-impossible to remove chondrules clean of matrix or fine-grained rims, or free of selection effects based on chondrule resilience to crushing.

The Semarkona (LL3.0) meteorite is widely regarded as the least metamorphosed, and thus "most primitive", ordinary chondrite (Dodd et al., 1967; Sears et al., 1980; Huss et al., 1981; Grossman and Brearley, 2005). It has highly heterogeneous mineral compositions, a "primitive" texture of highly diverse unaltered objects, no evidence for recrystallization of even the most sensitive phases, contains highly non-equilibrium assemblages, such as silicon-bearing metal (Rambaldi et al., 1980), and it has the lowest thermoluminescence sensitivity of any known ordinary chondrite (Sears et al., 1980).

About 35% (by number) of Semarkona chondrules are "reduced" (i.e. low FeO silicates, metal-bearing – 'A1' chondrules) and volatile depleted (relative to cosmic proportions), while about 60% of its chondrules are "oxidized" (i.e. high FeO silicate, metal-free – 'B1' chondrules) and contain CI proportions (Anders and Grevesse, 1989) of the volatile elements (Sears et al., 1992; Huang et al., 1996), The existence of two major types of chondrules has been recognized since Merrill (1920) and has been rediscovered through a variety of observations and recognized through a variety nomenclatures (see Sears, 2004). For Semarkona, at least, A1 chondrules are equivalent to the Jones (1994) Type I chondrules and B1 are their Type II chondrules, but the equivalency breaks down with chondrules from metamorphosed chondrites. Huang et al. (1996) and Sears et al. (1996) argued that the main difference in the history of group A1 and group B1 chondrules is the intensity of the flash-melting event that created them, and that while group A1 chondrules were reduced and lost virtually all of their volatile elements during formation, the group B1 chondrules did not.

Matsunami et al. (1993) discovered a large (~800 μm) group A1 chondrule in Semarkona which in most respects is a perfectly normal example of a group A1 chondrule, with a "mesostasis" (glassy groundmass) enclosing large grains of olivine crystals, sometimes called "phenocrysts". What made the Matsunami et al. chondrule noteworthy was that its mesostasis displays compositional zoning that is reflected in a distinct brightening of cathodoluminescence and thermoluminescence around the edges. The central regions of the mesostasis have 0.5 wt% Na while the outer regions reach ~2.0 wt% Na. This is the pattern for several other relatively volatile elements and, conversely, refractory elements are depleted in the outer regions of the mesostasis. It is now known that compositional zoning in the mesostasis of Semarkona group A1 chondrules is fairly common (DeHart et al., 1992; Grossman et al., 2002). Matsunami et al. (1993) suggested that volatiles lost from the chondrule during formation had recondensed and diffused into the chondrule during cooling. These chondrules clearly bear witness to the transport of Na and other volatile elements between the chondrule and its immediate surroundings.

Recent analyses have shown evidence for mass-independent fractionation of oxygen and sulphur isotopes in chondrules. These include the CV3 carbonaceous chondrite Mokoia (Jones et al., 2004), studies of chondrule chemistry and isotope systematics (Krot et al., 2006; Zanda et al., 2006), mass-independent fractionation of sulphur isotopes in Dhajala chondrules (Rai and Thiemens, 2007) and a new record for enrichment of ^{16}O of −75‰ in a chondrule from Acfer 094 (Kobayashi et al., 2003). Lyon et al. (1999) and Sears et al. (1999) presented evidence of non-mass-dependent fractionation of oxygen isotopes in the mesostasis of this Semarkona chondrule and corroboration that something interesting had happened to the oxygen isotope systematics in Semarkona chondrules was reported by Kita et al. (2007). Kita et al. report mass-independent fractionation of oxygen isotopes between the mesostasis and olivine and clinopyroxene phenocrysts, although they do not report mesostasis oxygen isotope ratios as light as values for the olivine phenocrysts reported in the present work.

In view of the interesting mass transport processes witnessed by this chondrule, and the complications surrounding measurements by bulk techniques, it seemed worthwhile to make a detailed study of the Matsunami et al. chondrule by ion microprobe, since this instrument can resolve spatial variations in isotopic composition on the scale of 10s of micrometers.

2. ANALYTICAL DETAILS

2.1. Description of the chondrule

The original chondrule section studied by Matsunami et al. (1993) was not available for ion microprobe studies

but these authors kindly provided the opposing cut face where its diameter was 400 μm compared with 800 μm diameter of the section studied by Matsunami et al. (1993) (Fig. 1). If we assume that the chondrule was spherical and that the Matsunami et al. section passed through the center of the chondrule then our section is offset by 345 μm. Fig. 1a shows a backscattered electron image of the chondrule showing a number of large olivine phenocrysts surrounded by a refractory mesostasis. It seems that ~50% by volume of the chondrule is olivine grains ranging in size from 10 μm to 100 μm and ~50% is mesostasis, so that available mesostasis areas are typically 30 μm across but reach ~120 μm by ~70 μm in one instance. Elemental data for the mesostasis were obtained using a Cameca SX100 Electron Microprobe at the University of Manchester using quantitative wavelength dispersive analysis along two perpendicular profiles (Fig. 1b). The results are shown in Table 1 and Fig. 2. The section of the chondrule studied here shows all the physical and compositional properties previously observed and discussed by Matsunami et al. (1993). Fig. 1c shows the locations at which ion microprobe data were obtained.

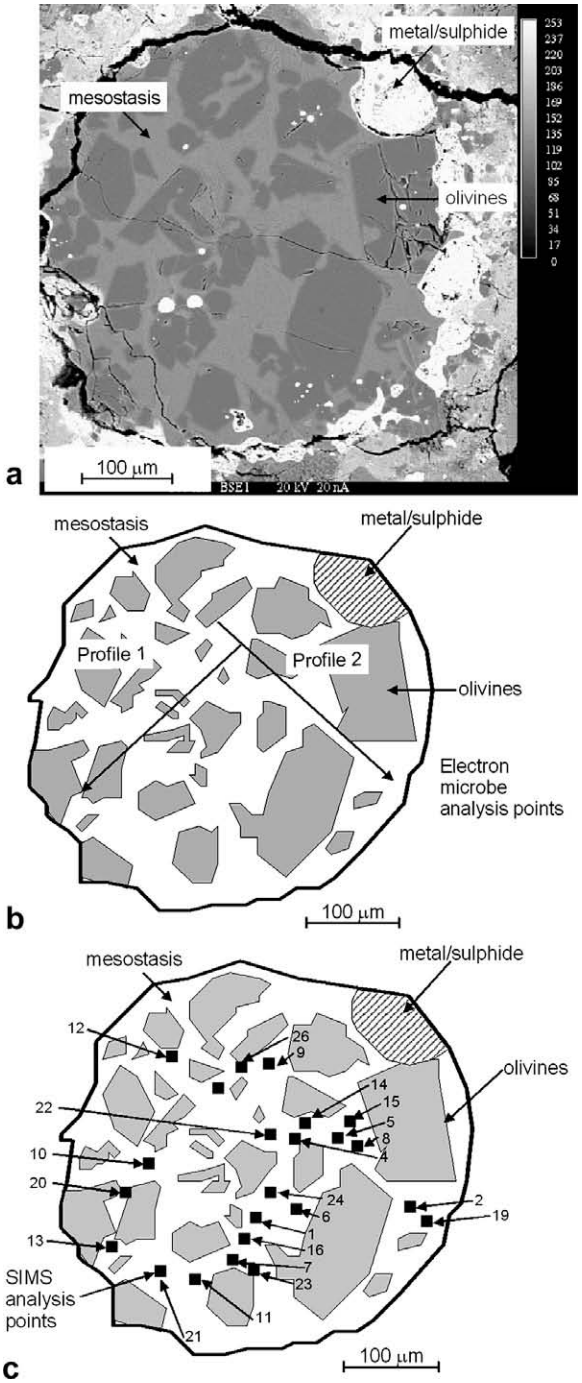

Fig. 1. Back scattered electron images of the chondrule from the Semarkona LL3.0 chondrite that is the subject of the present study. (a) The chondrule as it appeared originally. (b) Sketch showing the location of electron microprobe analyses (Table 1). (c) Sketch showing the location of ion microprobe analyses (Table 2). The sizes of the points analyzed are slightly smaller than the black squares in the sketch.

2.2. Ion microprobe analysis

Our oxygen isotope ratio analyses were acquired using the Manchester Isolab 54 ion probe. The instrument and procedures have been extensively described elsewhere (Saxton et al., 1996; Sears et al., 1998; Jones et al., 2000) but briefly: A 10 keV Cs^+ ion beam was focused to a ~15 μm diameter spot on the sample whose surface was held at −8 kV. An 18 kV (net 10 keV electron energy on the sample) electron beam a few 100 nA and a few 100 μm in size at the sample neutralized sample charging. The secondary ions were focused onto the source slit of a double-focusing mass spectrometer which passed the three oxygen isotopes into a multi-collector, using a Faraday detector for ^{16}O and conversion-dynode system multipliers (Saxton et al., 1996) for ^{17}O and ^{18}O. The ^{17}O beam was used for electrostatic peak centering. The mass resolution of our instrument was 6000 (10% peak height), sufficient to resolve ^{16}OH from ^{17}O. We also made a correction to the ^{17}O peak for overlap with the ^{16}OH peak, but this typically amounted to <1‰ in the $^{17}O/^{16}O$ ratio.

Glass standards of group A1 mesostasis composition were provided by Steve Symes and Gary Lofgren at the NASA Johnson Space Center by fusing mixed oxides. The 1σ scatter (for oxygen isotope ratios as measured, without normalization to any other standards or an average value of the ensemble of measurements) for $^{17}O/^{16}O$ and $^{18}O/^{16}O$ ratios on the glass standards were both about 1.4‰ on several hundred analyses obtained over periods of many months. This scatter includes all sources of error including variability of the CDS detectors used to measure the ^{17}O and ^{18}O currents relative to the Faraday detector used to measure the ^{16}O current. This value is therefore used as the 1σ confidence limit for a single oxygen isotope ratio analysis of an unknown material, provided that the unknown material has the same chemical composition as the glass standards. Standard measurements were interspersed with the sample measurements. We also analyzed four olivines in the present section for comparison with our earlier study, using olivine from the Brenham pallasite as a standard. The 1σ values for both $^{18}O/^{16}O$ and $^{17}O/^{16}O$ on the Brenham olivine were ~2‰.

Table 1
Elemental analyses of mesostasis in the Semarkona chondrule analyzed here for oxygen isotopes (expressed as oxides in wt%).

Point	Dist (μm)	Na_2O	MgO	SiO_2	Al_2O_3	K_2O	TiO_2	Cr_2O_3	CaO	NiO	FeO	MnO	Total
Profile 1													
1	0	1.38	5.59	52.07	20.30	0.01	1.19	0.60	17.22	0.03	0.64	0.15	99.18
2	36	1.44	4.77	51.88	20.03	0.02	1.22	0.60	17.27	0.04	0.40	0.20	97.85
3	71	1.52	5.96	56.23	19.35	0.04	1.01	0.46	16.23	0.02	0.33	0.17	101.32
4	80	1.54	5.58	56.08	19.69	0.03	0.99	0.47	16.23	0.02	0.39	0.18	101.20
5	88	1.56	5.59	55.55	19.30	0.09	0.93	0.41	16.14	0.00	0.40	0.16	100.14
6	101	2.13	5.28	55.78	19.34	0.03	0.96	0.47	15.69	0.00	0.97	0.28	100.92
7	130	1.99	5.42	55.95	19.32	0.07	0.93	0.36	15.58	0.03	0.49	0.13	100.28
8	110	2.42	4.88	56.11	19.22	0.07	0.95	0.38	15.77	0.03	0.76	0.14	100.71
9	131	2.39	5.35	58.11	18.07	0.09	0.91	0.40	14.99	0.01	0.56	0.24	101.12
10	131	2.34	5.27	58.42	18.24	0.08	0.92	0.30	14.97	0.02	0.62	0.13	101.31
11	142	2.54	4.96	59.25	17.68	0.13	0.83	0.22	14.16	0.12	1.61	0.16	101.67
12	150	2.88	4.59	60.23	18.08	0.11	0.83	0.27	13.93	0.07	0.69	0.16	101.82
13	137	2.31	5.13	58.27	18.38	0.05	0.82	0.30	14.36	0.00	0.47	0.23	100.33
14	141	2.33	4.66	59.60	18.78	0.11	0.84	0.21	14.19	0.00	0.50	0.15	101.37
Profile 2													
15	22	1.34	4.30	52.92	21.59	0.03	1.00	0.47	17.31	0.00	0.32	0.16	99.45
16	37	1.16	5.18	55.33	19.51	0.04	1.21	0.66	17.24	0.01	0.30	0.20	100.83
17	53	1.24	4.83	54.22	20.11	0.07	0.96	0.45	16.60	0.00	0.33	0.15	98.97
18	63	1.25	6.67	55.54	19.13	0.03	1.05	0.54	16.25	0.00	0.42	0.24	101.12
19	73	1.51	5.86	54.25	20.90	0.02	1.03	0.47	16.21	0.00	0.48	0.21	100.92
20	83	1.79	5.91	54.60	20.32	0.04	1.02	0.45	15.83	0.02	0.62	0.25	100.85
21	96	1.72	6.56	54.38	18.93	0.06	0.87	0.40	14.95	0.06	2.22	0.23	100.38
22	102	1.67	6.52	56.78	18.41	0.03	0.91	0.39	15.27	0.01	0.46	0.25	100.67
23	117	1.71	5.99	57.45	19.02	0.05	0.83	0.29	15.26	0.04	0.51	0.19	101.33
24	109	1.68	7.16	57.52	17.74	0.05	0.93	0.34	15.49	0.12	0.59	0.24	101.84
25	125	1.83	5.96	57.58	18.35	0.05	0.81	0.19	15.36	0.12	0.88	0.21	101.33
26	134	2.06	5.08	56.48	18.71	0.09	0.84	0.17	15.67	0.12	2.07	0.22	101.51

Our early results (Lyon et al., 1999; Sears et al., 1999) had shown an interesting correlation between oxygen isotope ratio composition and distance from the center of the chondrule. However, we subsequently discovered during extensive scrutiny and checking of our data for standards following the earlier results, that there was evidence for variable apparent width of the ^{17}O peak and furthermore, a small but significant correlation between measured $^{17}O/^{16}O$ ratio (to the level of 1–2‰) and the peak width. We deduced that the mass-defining slit for the ^{17}O detector was not quite parallel. This problem and its correction is described in the Appendix.

While correcting for a non-uniform slit width as discussed in the Appendix seemed straightforward, we also developed an independent method for making these measurements. Therefore, instead of moving the beam over the sample and varying the beam geometry relative to the slit, we connected the sample stage to a stepper motor and gearbox so that the sample stage could be moved and the beam geometry maintained. The process was automated by a microcontroller attached to the data acquisition computer and a series of 20-s measurements made by cycling a number of spots under the beam until counting statistics were acceptable. This method had an additional advantage that fluctuations in detector sensitivity average out, but has the disadvantage that sample coverage is limited and standards cannot be included in the sequence. Within experimental error, the oxygen isotope ratio slope found within the chondrule by the two methods are in agreement. Data from these two methods are presented below.

3. RESULTS

3.1. Data acquired by manually moving the sample and interspersing the sample analyses with standard analyses

As an additional quality control step we first measured the oxygen isotope composition of the large olivine phenocrysts present in the chondrule in order to compare them with our previously published results (Sears et al., 1998). Unfortunately, no peak shape monitoring data were obtained for these analyzes, and the slit correction cannot be applied, but the additional error resulting from this lack of correction is not thought to be more than 1‰, based on the agreement with our previously published data. The data appear in Table 2. The values we obtained were within about four permil of (0, 0) for $^{18}\delta O$ and $^{17}\delta O$, and randomly distributed, and very similar to our previous data for the large olivine grains in this chondrule. Our previously published data will also have been affected by the variable slit width problem. However, the data were acquired over an extended period involving multiple analysis sessions with new orientations of the section, so these errors would increase the scatter and not cause systematic differences between the earlier and the present data.

We analyzed 22 spots in the chondrule mesostasis (Fig. 1c) and the results are given in Table 2 and Figs. 3 and 4. The data have been corrected for detector dead-time, the slit width issue discussed in the Appendix, and normalized to V-SMOW values by comparison to the measured standards. The $\delta^{17}O$ values range from −2.0‰ to 9.9‰,

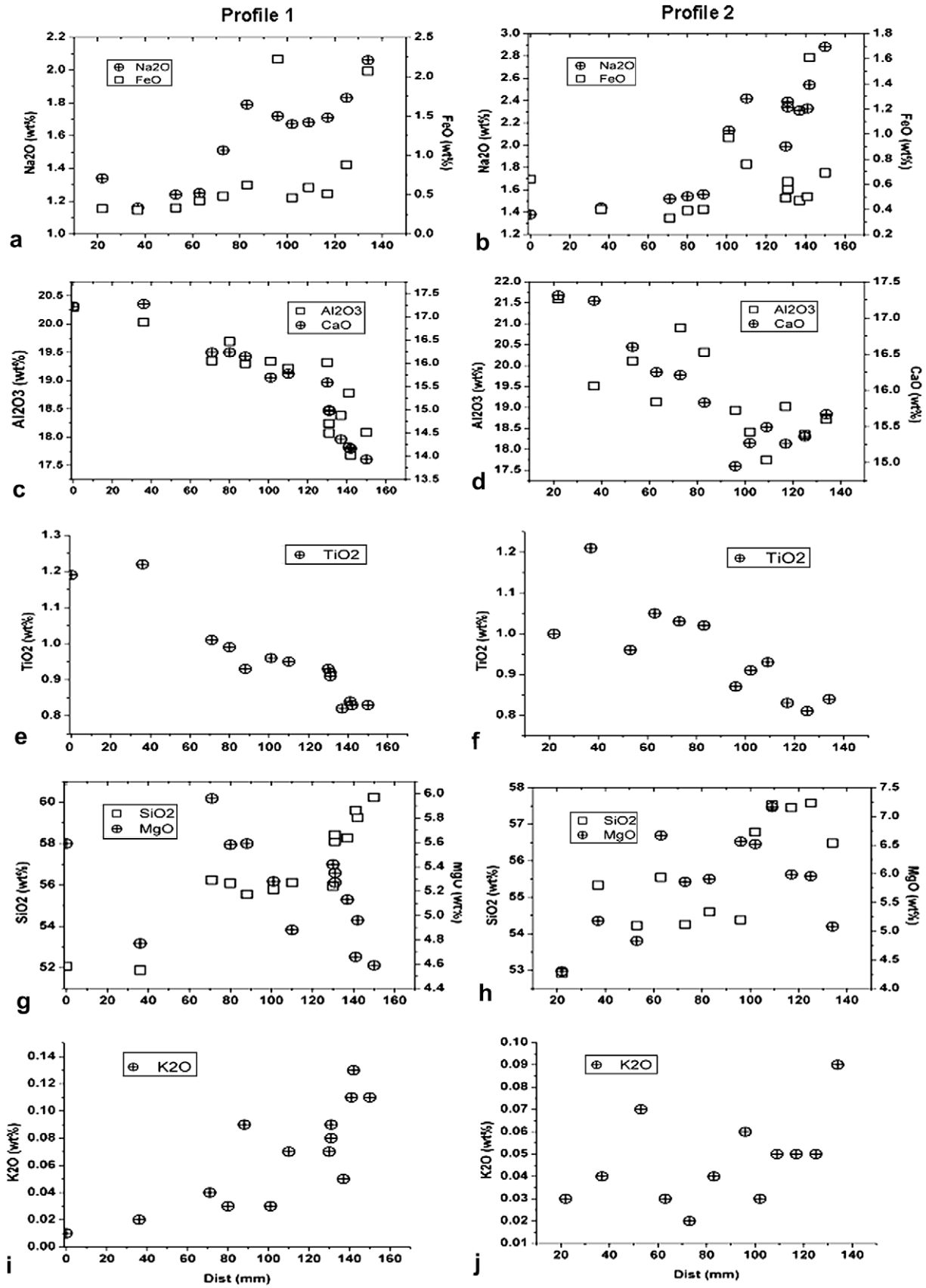

Fig. 2. Electron microprobe analyses of the mesostasis of the present Semarkona chondrule along the profiles shown in Fig. 1b. As observed for previous analyses of this chondrule by Matsunami et al. (1993), the mesostasis of this chondrule is compositionally zoned with the outer region being depleted in refractory elements and enriched in volatile elements relative to the central region.

Table 2
Oxygen isotope analysis results for chondrule mesostasis and olivine obtained by ion microprobe.[a]

Spot	$\delta^{17}O$ ‰ SMOW	$\delta^{18}O$ ‰ SMOW	$\Delta^{17}O$ ‰
Mesostasis analyses			
1	−1.9	−1.9	−1.0
2	1.9	5.0	−0.7
4	8.3	9.6	3.3
5	4.7	7.8	0.7
6	4.4	4.3	2.2
7	1.4	1.1	0.9
8	*(8.7)*	10.6	*(3.2)*
9	3.4	3.0	1.8
10	*(3.3)*	4.1	*(1.1)*
11	*(1.8)*	3.8	*(−0.2)*
12	*(−0.8)*	0.4	*(−1.1)*
13	1.6	1.6	0.8
14	9.9	7.5	6.0
15	7.7	7.2	3.9
16	−2.0	1.2	−2.6
19	4.7	8.9	0.1
20	2.9	1.6	2.0
21	2.4	4.0	0.3
22	8.2	8.3	3.9
23	3.4	6.9	−0.2
24	9.3	9.3	4.5
26	7.2	8.9	2.5
Olivine analyses			
1	(0.7)	−4.1	(2.8)
2	(0.0)	−1.2	(0.6)
3	(−3.0)	−3.9	(−1.0)
4	(−3.3)	1.1	(−3.8)

The 1σ values for both $^{18}O/^{16}O$ and $^{17}O/^{16}O$ on the Brenham olivine were ~2‰ and for the glass standards were ~1.4‰.

[a] The $\delta^{17}O$ values given in brackets and italics are uncorrected for the 'slit correction' (explained in the text) and are not used in the calculation of the slope looking at the co-variation of $\delta^{17}O$ with $\delta^{18}O$.

while $\delta^{18}O$ range from −1.9‰ to 9.6‰. Measurements of ^{17}O peak width obtained during peak centering were not available due to failure of electronic data transfer during acquisition for spots 8, 10, 11 and 12 so we were not able to apply the peak width correction to $\delta^{17}O$ values for these spots. The $\delta^{17}O$ values for these spots in Table 2 are therefore shown in brackets and have not been used to calculate the slope of the correlation line between $\delta^{18}O$ and $\delta^{17}O$ in Fig. 3 (although any correction to the $\delta^{17}O$ values are not likely to have been more than ~1‰). These data points are shown in Fig. 3 as gray squares and do not deviate significantly from the regression line defined by the corrected data points.

A least squares fit line through the data which takes into account the experimental uncertainties in the data has a slope of 0.88 ± 0.10 (1σ). The $\delta^{18}O$ and $\delta^{17}O$ values do not vary randomly with position; but the highest $\delta^{18}O$ and $\delta^{17}O$ values are mostly found in the central region of the chondrule while lower values are found in the outer regions (Fig. 4b). In other words, the chondrule mesostasis is

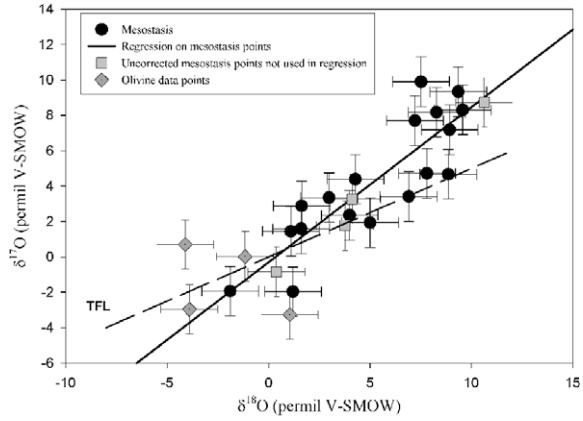

Fig. 3. $\delta^{17}O$ against $\delta^{18}O$ for the mesostasis of the chondrule. The regression line through the present data has a slope of 0.88 ± 0.10. Also shown is the line terrestrial fractionation line (TFL) (slope ~ 0.52) from Clayton et al. (1991). Typical 1σ uncertainties for the present data are shown.

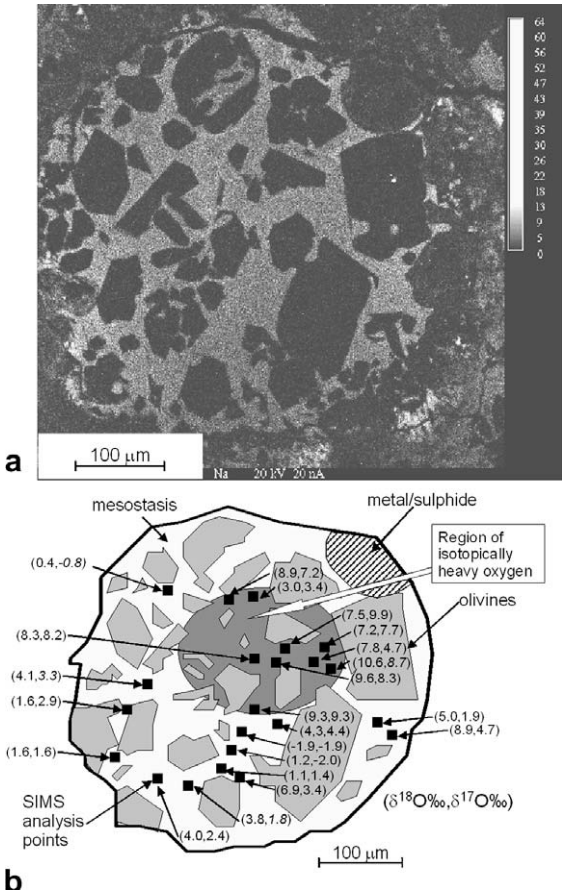

Fig. 4. Comparison of the zoning in the present chondrule. (a) Na X-ray image of the chondrule showing the sodium enrichment in the outer regions of the chondrule. (b) Distribution of oxygen isotope values ($\delta^{18}O$‰, $\delta^{17}O$‰) with the area of heavy oxygen indicated. Values in italics have not been corrected for certain instrumental effects. The refractory central regions of the chondrule mesostasis contain isotopically heavier oxygen than the outer regions.

zoned in oxygen isotopes, as it is in elemental composition (Figs. 2 and 4a), but remarkably, the $\delta^{18}O$ and $\delta^{17}O$ values plot along a line that within experimental error is significantly different from the mass-dependent fractionation slope of ~0.52.

There is a correlation between oxygen isotope composition and radial location in the chondrule with mesostasis in the center of the chondrule being isotopically heavier than mesostasis towards the outer edge of the chondrule. This is illustrated in Fig. 4b.

3.2. Data acquired by mechanically stepping the sample between two different spots on the sample

The measured $^{18}O/^{16}O$ and $^{17}O/^{16}O$ ratios for three runs, each of four spots on the A1 glass standard are presented in Table 3. These data confirm that the precision of both our $^{18}O/^{16}O$ and $^{17}O/^{16}O$ ratios is limited only by counting statistics. The same sequence of analyses were acquired on the mesostasis of the chondrule with some spots being within the outer mesostasis and others being near the center. Because there was such limited movement possible with the sample stepper motor system, it was not possible to intersperse analyses of the chondrule with analyses of the standard using this method. The results for the sample shown in Table 4 are therefore not absolute (relative to V-SMOW) oxygen isotope ratio values but are calibrated relative to the mean observed ratio. The important quantity that we wished to derive from this sequence of analyses was the slope of the $\delta^{17}O$ versus $\delta^{18}O$ line to compare with our previous measurements.

The spots labeled 23rd May in Table 4 did not properly sample the span of mesostasis position that we intended and show olivine data as well as results from mesostasis for the outer part of the chondrule. After inspection of the chondrule in an SEM to determine the sampled areas, we obtained further data on 1st June and these spot pairs successfully spanned the mesostasis in the center of the chondrule and the mesostasis near the edge. Oxygen isotope values reported here are relative to the mean value for that day and cannot be compared in absolute value with data reported in Table 2 that are normalized to V-SMOW. The measured relative oxygen isotope ratios may however be used to determine the relative values between the measured spots during a single run. The slope of the $\delta^{17}O$ versus $\delta^{18}O$ line for the spots on the inner mesostasis compared with the outer mesostasis is 1.1 ± 0.2 (1σ), independently confirming our previous measurements that the slope is significantly different from ~0.52 predicted for mass-dependent fractionation.

Table 3
Oxygen isotope data from standard glass obtained by ion microprobe multi-spot analysis.

Date	$^{17}O/^{16}O$ 1σ actual ‰	$^{17}O/^{16}O$ 1σ expected[a] ‰	$^{18}O/^{16}O$ 1σ actual ‰	$^{18}O/^{16}O$ 1σ expected[a] ‰
30-4-01	1.2	1.0	0.3	0.4
1-5-01	1.3	1.4	1.4	0.6
2-5-01	0.9	1.2	0.5	0.5

[a] "Expected values" are those determined by A.E. Fallick (Scottish Universities Environmental Research Centre) using bulk techniques.

Table 4
Oxygen isotope ratios for chondrule olivines and mesostasis obtained by ion microprobe multi-spot analysis.[a]

Date	Spot	$\delta^{17}O$ (‰)	$\delta^{18}O$ (‰)	$\Delta^{17}O$	Material
23	1	2.0 ± 1.7	4.4 ± 0.7	−0.3	Mesostasis[b]
May	2	-2.0 ± 1.5	-4.6 ± 0.6	2.0	Olivine
	3	1.4 ± 1.7	3.8 ± 0.8	−0.5	Mesostasis
	4	-4.7 ± 1.4	-3.6 ± 0.6	−1.2	Olivine
1 June	1	3.6 ± 0.9	3.2 ± 0.3	1.8	Heavy mesostasis
	2	-3.6 ± 0.8	-3.2 ± 0.4	−1.8	Mesostasis[b]

[a] Each data set has an arbitrary zero point. The olivine-glass matrix effect is included. See text for further discussion.

[b] 23 May point 1 and 1 June point 2 sampled same region of mesostasis.

3.3. Data summary

To summarize our ion microprobe data: (i) The olivines have more ^{16}O-rich oxygen isotopic values than the mesostasis (Fig. 3). (ii) As with elemental composition, the mesostasis is compositionally zoned in oxygen isotopes ($\delta^{18}O$, $\delta^{17}O$) being about (0‰, 0‰) in the outer regions and (+10‰, +8‰) in the central region (Fig. 4); (iii) On a plot of $\delta^{17}O$ versus $\delta^{18}O$, the mesostasis analyses plot along a line with a slope of 0.88 ± 0.10 (1σ), which is significantly different from ~0.52 (Fig. 4).

4. DISCUSSION

We will not discuss at length the nature of the elemental profiles in the chondrule mesostasis and their causes except to observe that the present section shows the same properties as the section of the same chondrule described by Matsunami et al. (1993) and the same interpretations apply. Fig. 2 shows the compositional profiles and Fig. 4 shows images of this chondrule by Na X-rays, and measured $\delta^{18}O$ and $\delta^{17}O$ values. Just as the chondrule is zoned in elemental analysis, with volatile elements enriched near the perimeter (Fig. 2), the mesostasis in the periphery is ^{16}O enriched. Fig. 4 compares the areal extent of the Na-enriched regions and the region of heavy oxygen.

The Na/Al ratios for the mesostasis range between 0.08 and 0.24 and K/Al ratios range between 0.01 and 0.17 (Table 1). The Na/Al and K/Al show a positive correlation. Grossman and Brearley (2005) following Grossman et al. (2002) presented data showing that mesostasis in Semarkona chondrules followed a trend between very low K/Al and Na/Al values (~0.01 and 0.1, respectively, for unmetamorphosed and unaltered chondrules) up to values of 2.5 and 1, respectively, for metamorphosed and altered chondrules. Our data for this chondrule places the mesostasis as unmetamorphosed and unaltered.

Finally we note here the ample evidence that this chondrule has not suffered any form of aqueous alteration. First, the mesostasis around the edges of the chondrule is optically clear glass, with no sign of the formation of hydrous silicates noted by Hutchison et al. (1987). Second, our electron microprobe analyses sum to 100%, Hutchison et al. (1987) found values as low as 77.9%, reflecting the presence of ~20% of water undetectable by the microprobe. Third, thermoluminescence and cathodoluminescence is highly susceptible to aqueous alteration and quickly diminish below detectable levels where as we see an increase in the intensity of these near the edges of the chondrule.

Matsunami et al. considered the following possible explanations for the elemental zoning:

- Differences in the degree of olivine crystallization during cooling. This was ruled out because of the detailed nature of the elemental trends and textural uniformity of the olivine.
- Element migration along steep temperature gradients, which was again ruled out because of the detailed nature of the elemental trends.
- Elemental transport during aqueous alteration was eliminated because of the lack of petrographic evidence for aqueous alteration and analytical sums of 100% during quantitative electron probe micro-analysis. Subsequent work (Grossman et al., 2002; Grossman and Brearley, 2005) has shown evidence for aqueous alteration in some Semarkona chondrules. However, our analyses are in agreement with the Matsunami et al. (1993) data and confirm that there was no aqueous alteration of this chondrule.
- Zoned precursor materials were thought unlikely because the mesostasis is a contiguous phase that was once entirely melted. There were also elemental trends that seemed inconsistent with this idea.
- A mechanism involving reduction of precursor aggregates was eliminated because diffusion rates are too small for this to occur on the timescale of chondrule formation.
- Element transport into the chondrule by diffusion following recondensation of previously evaporated components appeared to be consistent with elemental trends, quantitative considerations and laboratory experiments. The characteristic diffusion length $(Dt)^{1/2}$, for Na in a glass at the melting point is 66 μm for 1 s and 510 μm for 1 min, assuming a diffusion coefficient of 4.3×10^{-5} cm^2/s (Young et al., 1998). Thus a chondrule liquid phase of just a few seconds seems required for a chondrule immersed in a volatile-rich gas to acquire these compositional profiles in its mesostasis. Many authors have demonstrated in the laboratory how volatile elements can escape from chondrule-like silicate mixtures at elevated temperatures (Sears, 2004; Alexander and Grossman, 2005). The order of loss in a reducing atmosphere follows the expected thermodynamics, Na, then K, then FeO is reduced to Fe which is lost, then Si is lost and finally Mg. It has also been demonstrated in laboratory experiments that Na can readily reenter an experimental charge it has previously escaped from as conditions change (Lewis et al., 1993).

There has also been much work on isolated olivine phenocrysts in chondrules with a view arising that some are actually relic grains from a previous generation of chondrule formation, often retaining ^{16}O-rich compositions (Saxton et al., 1995, 1998; Jones et al., 2000; Krot et al., 2006; Zanda et al., 2006; Libourel et al., 2008). Young et al. (2002) show that there are olivines within chondrules that resemble relic grains and that are ^{16}O-rich relative to mesostasis. It is possible that this is a wide-spread feature. We are of the view however that the petrographic evidence suggests that the olivine phenocrysts in this chondrule crystallized from a completely molten droplet, for the reasons explained by Matsunami et al. (1993), with the help of nucleation centers too small to affect mass balance. Not only does the composition suggest peak temperatures during chondrule formation in excess of the liquidus temperature, but melt-solid distribution coefficients are consistent with crystallization from a melt. At the same time, the olivines in this chondrule lack any of the properties associated with relic grains, such as anomalous compositions or evidence for reaction between the grain and the mesostasis.

These observations and deductions being so, it seems reasonable to ask whether the mass transport associated with chondrule formation involved isotopically unusual oxygen and whether oxygen isotope ratio measurements of this chondrule can yield further insight into the chondrule-forming process.

From the earlier discussion of mechanisms that can produce non-mass-dependent isotopic fractionation of oxygen isotopes we can envisage several scenarios that can potentially account for the observed isotopic systematics and elemental patterns of this chondrule: these are described schematically in Fig. 5.

(a) Prior to the formation of the chondrule there existed a mixture of olivine and mesostasis precursors that were depleted in volatile elements and differing in oxygen isotopes in a non-mass-dependent fashion, the olivine precursors being ^{16}O-rich and the mesostasis precursors being ^{16}O-poor. How these properties came about we consider outside our purview, although mechanisms like self-shielding either in the early solar nebula, or the parent molecular cloud, are possible with volatile depletions arising because of either a heating event like impact, or accretion at high temperatures. These components were flash melted into a chondrule without changing their properties. While still hot, the chondrule became immersed in a gas containing ^{16}O-rich oxygen and volatile elements that diffused into the outer regions of the mesostasis. This process could have occurred in the nebula phase, prior to accretion of the parent body of the chondrites.

(b) The same combinations of precursors and events as scenario (a) can be envisaged but the instead of the hot chondrule being embedded in the nebular cloud, we can imagine that the hot chondrule was buried in a regolith on the parent body where it interacted by an aqueous fluid containing ^{16}O-rich material and volatile elements.

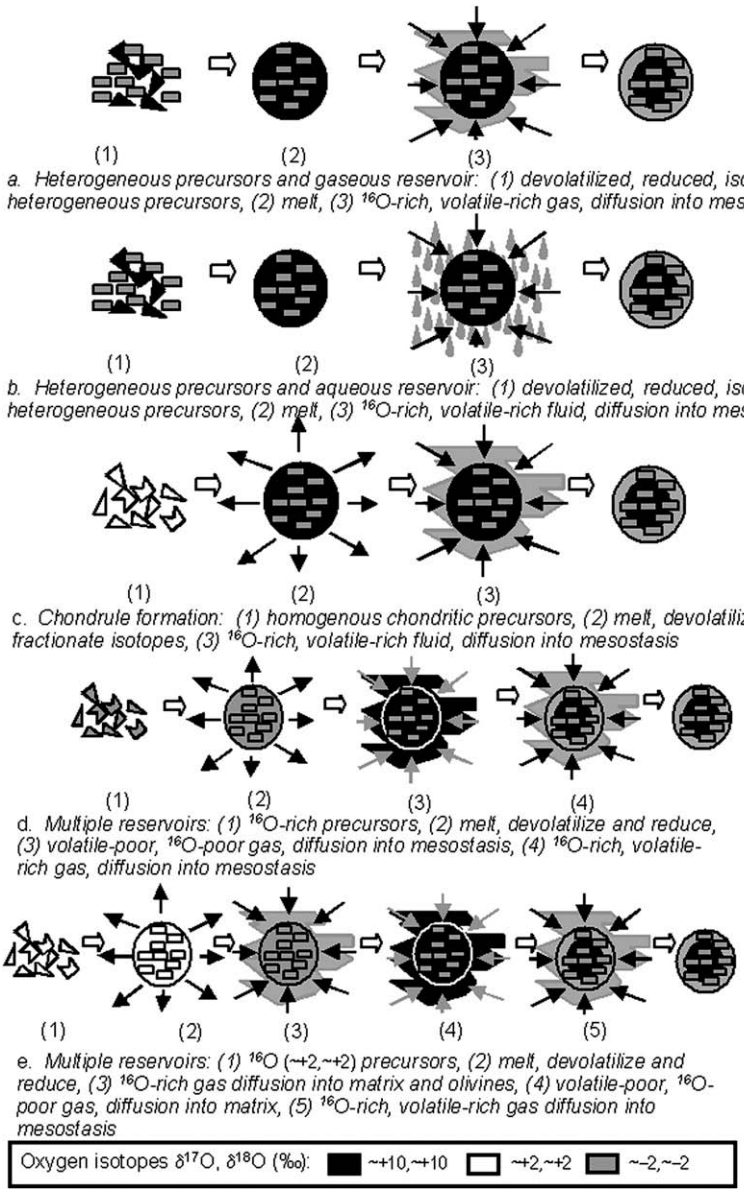

Fig. 5. Schematic representations of five scenarios by which the oxygen isotopic, petrographic, and compositional properties of the present chondrule could have been achieved. Scenarios (a) and (b) assume that the chondrule precursors were heterogeneous, volatile poor, and oxygen in the components fractionated relative to each other by mass-independent means. The volatile elements and ^{16}O-rich oxygen were then introduced to the chondrule from the gaseous environment or by aqueous alteration. Scenario (c) assumes chondritic precursor materials and that most of the properties of the chondrule were achieved during chondrule formation with volatiles and ^{16}O-rich oxygen back reacting with the chondrule during cooling. Scenarios (d) and (e) achieve the properties of the present chondrule by exposure to multiple different environments, two environments being required if the precursors were ^{16}O-rich, three were required if the precursors were chondritic. We argue in favor of scenario (c) since it is simplest in terms of number of events and number of environments, assumes chondritic precursors, and it is consistent with the petrography and composition of the chondrule. We argue that the other scenarios are not consistent with the petrography and composition of the chondrule and sometimes require an unlikely combination of events. On the other hand, scenario (c) suggests that crystallization of phenocrysts in the chondrule melt resulted in mass-independent fractionation of the oxygen isotopes, a process that seems plausible in view of recent empirical and theoretical work on mass-independent oxygen isotope fractionations.

(c) Precursor grains with chondritic abundances, including volatile components, and intermediate oxygen isotope composition were flash melted into a melt spherule which cooled to produce olivine phenocrysts and feldspathic mesostasis. During this process volatiles were lost, the chondrule was reduced, and oxygen was fractionated in a mass-independent way, the olivines becoming ^{16}O-rich and the mesostasis ^{16}O-poor. As the object cooled, it was immersed in a cloud of material made of the volatile elements and oxygen-bearing species produced by the heating event, and these back-reacted with the chondrule to

form the outer mesostasis zone that is ^{16}O-rich and high in volatiles. Thus virtually all the elemental and isotopic properties of the chondrule are attributed to the chondrule-forming process and subsequent cooling. Oxygen isotopes are fractionated in a mass-independent way by crystallization of the phenocrysts in the melt. In terms of the oxygen three-isotope diagram, this scenario is described in Fig. 6. This scenario requires the hypothesis that the chemical reactions within the molten chondrule can mass-independently fractionate oxygen isotopes in an analogous way to known mechanisms discussed by Thiemens et al. (1996), Thiemens (2006), Kimura et al. (2007) and Ali and Nuth (2007).

(d) ^{16}O-rich precursors are melted by a flash-heating event and cooled to produce phenocrysts, without any change in isotopic composition but with the lost of volatiles and reduction. Thus the olivine grains and the mesostasis are ^{16}O-rich. This chondrule was immersed in a ^{16}O-poor reservoir, which diffused into the mesostasis without affecting the olivines. The chondrule was then exposed to a second and different ^{16}O-rich gaseous reservoir and volatiles, which diffused onto the outer regions of the mesostasis.

(e) Our final scenario for creating the present chondrule is the same as (d) except that we start with precursors of chondritic composition and intermediate oxygen isotope composition. After formation of the chondrule by the flash-heating event during which the volatile were removed and the chondrule was reduced, the hot chondrule was immersed in an ^{16}O-rich vapor that diffused throughout the chondrule olivines and mesostasis. Thereafter the scenario is the same as (d).

Scenarios (a) and (b) attribute the most critical properties of the chondrule, the loss of volatiles and, more

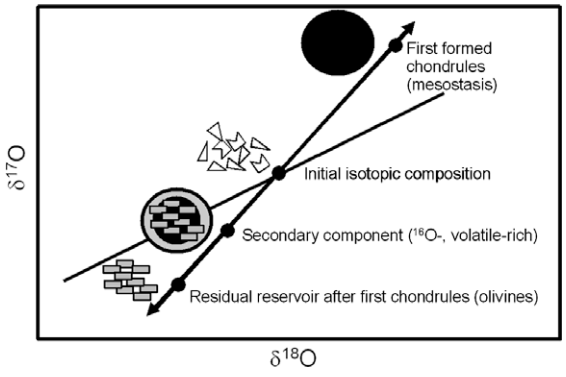

Fig. 6. Scenario (c) production of the elemental and oxygen isotopic properties of this chondrule during chondrule formation and back-reaction during subsequent cooling expressed in terms of an oxygen three-isotope plot. Precursor grains with chondritic properties are melted during chondrule formation and the melt crystallizes to produce phenocrysts that are ^{16}O-rich and mesostasis that is ^{16}O-poor and fractionated mass-independently relative to each other. At this point the chondrule is devolatilized and reduced. Back reaction of the chondrule with the gases released on heating produce the isotopic and compositional zoning observed in the chondrule.

especially, the mass-independent fractionation of oxygen between olivine grains and feldspathic materials that were to become mesostasis, to nebular and/or parent body processes. Either of the previously discussed mechanisms for chemical fractionation – self-shielding or surface–gas interactions – might apply to processes occurring in the nebula prior to chondrule formation. What is important, is that mineralogical differentiation occurs during isotope fractionation. The most frequent method for separating feldspathic phases from mafic phases is melt formation and crystallization, but one might imagine fractional condensation or evaporation processes would also work. The weakness of scenarios (a) and (b) is that they are not consistent with the petrography of this chondrule and with our conviction that this object was entirely molten during formation, that the olivine grains are phenocrysts that formed by crystallization, not relic grains, and that this object has not suffered aqueous alteration.

The third scenario is the simplest in that it involves chondritic precursors, few steps, and few environments. In fact, since the ambient gas is produced by the chondrule-forming event, it essentially is a single environment, multi-phase but single step process. However, it involves proposing a new process for mass-independent oxygen isotope fractionation, namely crystallization from a melt. It might be that some of the statistical arguments used by Marcus (2004) to describe mass-independent isotope fractionations on the gas–solid interface might apply at the melt-solid interface. The strength of scenario (c) is that it is consistent with the petrography and composition of this chondrule as described and discussed in some detail by Matsunami et al. (1993).

Several types of symmetry-selective chemical reaction lead to mass-independent fractionations, addition reactions, gas phase isotopic exchange, thermal decomposition or exchange of an oxygen atom with CO_2. Thiemens (1996) proposed that reactions such as:

$$O^* + OSiO = O + OSiO^*$$
$$O(^1D) + CO_2 \Longleftrightarrow CO_2{}^*$$
$$CO_3{}^* + \rightarrow CO_2 + O(^3P)$$

and many others occurring during open system chondrule formation will all lead to slope-one lines on the δ^{17}O versus δ^{18}O plot. These processes produce ^{16}O-poor chondrules and an ^{16}O-rich residual solid (Fig. 5d).

A chemical process that produces mass-independent fractionation of oxygen isotopes during CAI formation has been proposed by Marcus (2004). While we stress that there are differences as well as similarities between his work and our proposed scenario, his observations prompt us to consider an analogous mechanism for explaining oxygen isotope systematics during chondrule formation. The factor that induces the apparent asymmetry between ^{16}O and the two heavier isotopes ^{18}O and ^{17}O arises because of the naturally high abundance of ^{16}O (~99.8%) compared with ^{18}O (~0.2%) and ^{17}O (~0.038%). Any molecule that contains two oxygen atoms is highly unlikely to contain two ^{17}O atoms or two ^{18}O atoms. In a quantum system such for the molecules discussed here, differences in the number of

allowed states in molecules arise when two of the atoms are identical compared to when the two atoms are not identical. ^{17}O and ^{18}O have such low natural abundances that in nearly all of the molecules analyzed, the abundance comparisons are between $^{16}OX^{16}O$ and $^{16}OX^{17or18}O$ where X is a cation such as Si or Al in the case of CAIs and Mg or Fe in the case of chondrules. In a highly dynamic situation such as for reactions like $OX_{abs} + O \leftrightarrow OXO_{abs}$, which are occurring on the surface of a growing miniature body such as a CAI or chondrule, the position of the equilibrium point can be different for symmetric and asymmetric molecules. The symmetry of the $^{16}OX^{16}O$ molecule results in some forbidden quantum states that are allowed for molecules with $^{16}OX^{17or18}O$. The former therefore has a poorer density of vibrational quantum states compared to the latter asymmetric molecules and a longer lifetime for dissociation. This makes it more amenable to collisional de-excitation to form the solid OXO. Mass-independent fractionation therefore occurs for ^{16}O compared with $^{17,18}O$.

There is now good experimental evidence that the formation of solids can involve mass-independent fractionation of oxygen isotopes (Thiemens, 2006; Ali and Nuth, 2007; Kimura et al., 2007) so the formation of the chondrule could have induced mass-independent fractionation in its components with subsequent recondensation of some of the material bringing back more ^{16}O-enriched and volatile-enriched composition to the outer part of the chondrule. However, it is still difficult to envisage how the olivines acquired their ^{16}O-enriched composition if they were formed by crystallization from a melt, which was ^{16}O-poor, having acquired that composition from the chondrule-forming process. A possibility is that mass-independent fractionation reactions can also occur within a liquid. All the chemical reactions studied so far that show mass-independent fractionation behavior has been gas phase or gases condensing onto solid surfaces but may be these mechanisms are extendable into other phases.

Exposing the chondrule to multiple environments as in scenarios (d) and (e) can also explain the elemental and isotopic properties of this chondrule, but two independent environments are required if the precursors are enriched in ^{16}O, and three are required if the precursors are chondritic. We find these scenarios somewhat contrived. It is not clear how the different environments would be created, and – most important – these scenarios are not consistent with the petrography and composition of the chondrule that suggest complete melting with subsequent crystallization of the olivine phenocrysts. We also argue that if the species bringing in the ^{16}O-rich material at the end of the sequence of events was water, that there would be clear indications of aqueous alteration.

In short, we consider all the properties of this chondrule – petrographic, mineralogical, compositional, and isotopic – to be best explained in terms of scenario (c), requiring a method of mass-independent isotope fractionation that, while analogous to previous suggestions, has not previously been discussed.

5. CONCLUSIONS

We have analyzed oxygen isotopes in a group A (Type 1) chondrule from the Semarkona meteorite. There is strong petrological evidence that the chondrule material was completely molten during chondrule formation and that olivine phenocrysts crystallized from the melt leaving glassy mesostasis, which solidified without further change. The olivine phenocrysts have ^{16}O-enriched oxygen, the inner mesostasis has ^{16}O-depleted oxygen and the mesostasis in the outer rim of the chondrule has ^{16}O-enriched oxygen. We have sought here to understand how this pattern of oxygen isotope composition could arise and what light it may shed upon chondrule formation.

There are two main mechanisms by which oxygen can undergo non-mass-dependent fractionation. (i) Formation of reservoirs in the early solar system or its precursor molecular cloud which are mass-independently fractionated relative to each other. The mechanism for the isotopic fractionation being photochemical self-shielding by CO molecules. (ii) Mass-independent isotopic fractionation occurs through symmetry based selection during chemical reactions. This mechanism would lead to more localized, fine-scale variation in oxygen isotope fractionation than the external reservoir scenario. Preliminary measurements of the oxygen isotope composition of solar wind implanted into collectors recovered from the Genesis mission suggest that the sun may be significantly mass-independently fractionated relative to much of the solid material observed in the remainder of the solar system, thus giving support for the model with large separate oxygen reservoirs.

We examined both of these mechanisms for producing the detailed isotopic systematics observed in this Semarkona chondrule and have been unable to formulate a satisfying way in which either can account for the details observed. Petrological evidence suggests that the chondrule material was completely molten and that the olivine phenocrysts were formed by crystallization from the melt, the remaining material forming a solid glassy mesostasis. There is no evidence for relic grains or aqueous alteration in this chondrule.

It is clear that most chondrules had a complex, probably multi-step history. We have found a single chondrule which is of a type that is widely assumed to have been completely melted and devolatilized (Scott and Taylor, 1983; Sears et al., 1996), that has suffered some reentry of volatiles and that contains mesostasis with an oxygen isotope fractionation that is not mass dependent. We have considered five scenarios by which these properties could have been obtained. We conclude that the simplest scenario that is most consistent with its oxygen isotope systematics and its petrographic and compositional properties is that these properties were created during chondrule formation, crystallization, and subsequent cooling. Thus we propose that crystallization from a melt can produce mass-independent fractionations of oxygen isotopes. It is at least arguable that mass-independent fractionations so often observed in chondrite material may in some way be associated with chondrule formation.

ACKNOWLEDGEMENTS

We are grateful to Kiyotaka Ninagawa of the Okayama University of Science for providing the polished section of the Semarkona chondrule used in this work, Dave Blagburn and Bevest Clementson for help in maintaining the instrument, Grenville Turner for support, encouragement, and discussion, Gary Lofgren of the Johnson Space Center and Steve Symes (then at JSC but now at the University of Tennessee, Chatanooga) for providing glass standards, David Plant for assistance in obtaining the EPMA analyses of the chondrule, A.E. Fallick (Scottish Universities Environmental Research Centre) for O isotope determinations of glass standards, and the UK. Particle Physics and Astronomy Research Council (now Science and Technologies Facilities Council) and US National Science Foundation (INT program) for providing the funds to support this work. We are also grateful to Hazel Sears for reviewing and checking the paper. Finally, we are indebted to three anonymous reviewers and the Associate editor Sara Russell who provided very detailed and constructive comments on earlier versions of the paper.

APPENDIX A

As stated in the main text, a systematic variation of $^{17}O/^{16}O$ ratio with ion beam position on the sample was suspected. This results in some small corrections (of up to 1–2‰) to data presented here and hence some small differences with data published previously in abstracts (Lyon et al., 1999; Sears et al., 1999). The effect results from an inferred slight tapering of width with height of the slit in front of the ^{17}O detector.

The defining slit in front of the ^{17}O detector was set to 90 μm and the variation in width amounted to a decrease of a few microns in moving several millimeters along the line of the slit from the center vertical line of the instrument. In order to explain what effect this may have had on the data and how we have corrected our data, we expand upon this below.

To ensure complete accuracy in acquiring isotope ratio measurements, it is necessary that an ion beam enters the detector with 100% transmission through the mass-defining slit in front of the detector. The condition for this requirement is that the ion beam width should be much smaller than the detector slit. In oxygen isotope ratio measurements, this condition is most stringent for analyses of ^{17}O since a mass resolution of ~6000 is required to adequately resolve ^{17}O from the major ^{16}OH interference and because $^{17}O/^{16}O \sim 3.8 \times 10^{-4}$ so that the $^{17}O^-$ beam current is small, perhaps a few hundred counts per second. To acquire better than 1‰ precision on measuring $^{17}O/^{16}O$ ratios requires $>10^6$ acquired counts of ^{17}O so with the ^{17}O beam, in practice it is nearly impossible to verify the complete transmission of the ^{17}O beam into the detector to an accuracy of 1 part in 1000 under realistic analytical conditions. A slight loss of transmission into the detector will not matter if it is always the same for every analysis. This could be true if the detector defining slit is completely parallel and the peak is accurately centered upon the slit for every measurement. If the defining slit is not completely parallel however, and the ion beam enters the detector at different places along the slit for different analyses, then there may be a slight loss of transmission into the detector where the slit is narrower. A drop from 100% to 99.9% transmission directly translates into a 1‰ change in the measured $^{17}O/^{16}O$ ratio, an amount equal to the confidence limit on the measurement. There would also be no problem if the ^{17}O beam entered the detector at exactly the same slit width each time, but we found that this may not necessarily have been the case.

A slightly different ion beam trajectory around the instrument (such as is caused when the primary ion beam is steered to a different spot on the sample for analysis of a different area) can cause the secondary ion beam to fall on a different part of the mass-defining slit in front of the detector. Fortunately we used the ^{17}O ion beam for electrostatic beam centering and routinely monitored and recorded the apparent width of the ^{17}O peak during nearly every single $^{17}O/^{16}O$ ratio measurement including the extensive measurements on standards. We found that there was a slight correlation between measured $^{17}O/^{16}O$ ratios against ^{17}O peak width from the extensive standards data. We used this correlation and the beam monitoring data for $^{17}O/^{16}O$ and $^{18}O/^{16}O$ analyses on the sample to correct the $^{17}O/^{16}O$ ratios for measurements on the chondrules. The correction typically amounted to between 0‰ and 2‰ in the measured $^{17}O/^{16}O$ ratios making our data reported here, slightly different from those reported by Lyon et al. (1999) and Sears et al. (1999).

REFERENCES

Alexander C. M. O. and Grossman J. N. (2005) Alkali elemental and potassium isotopic compositions of Semarkona chondrules. *Meteorit. Planet. Sci.* **40**(4), 541–556.

Ali A. and Nuth J. A. (2007) The oxygen isotope effect in the earliest processed solids in the solar system: is it a chemical mass-independent process? *Astron. Astrophys.* **467**(3), 919–923.

Anders E. and Grevesse N. (1989) Abundances of the elements: meteoritic and solar. *Geochim. Cosmochim. Acta* **53**, 197–214.

Boss A. P. (1996) Large scale processes in the solar nebula. In *Chondrules and the Protoplanetary Disc*, vol. 257 (eds. R. H. Hewins, R. H. Jones and E. R. D. Scott). University of Cambridge Press, pp. 29–34.

Bridges J. C., Franchi I. A., Sexton A. S., Hutchison R. and Pillinger C. T. (1998) Correlated mineralogy, chemical compositions and sizes of chondrules. *Earth Planet. Sci. Lett.* **155**, 183–196.

Bridges J. C., Franchi I. A., Sexton A. S. and Pillinger C. T. (1999) Mineralogical controls on the oxygen isotopic composition of UOCs. *Geochim. Cosmochim. Acta* **63**, 945–951.

Chakraborty S. and Bhattacharya S. K. (2003) Mass-independent isotopic fractionation: recent developments. *Curr. Sci.* **84**(6), 766–774.

Chakraborty S., Ahmed M., Jackson T. L. and Thiemens M. H. (2008) Experimental test of isotope self-shielding in VUV photodissociation of CO. *Lunar and Planetary Science Conference.* #1145.

Clayton R. N. (2002) Solar system – self-shielding in the solar nebula. *Nature* **415**(6874), 860–861.

Clayton R. N. (2008) Oxygen isotopes in the early solar system – a historical perspective. In *Oxygen in the Solar System*, (Reviews in Mineralogy and Geochemistry, vol. 68), Mineralogical Society of America, pp. 5–14.

Clayton R. N. and Mayeda T. (1984) The oxygen isotope record in Murchison and other carbonaceous chondrites. *Earth Planet. Sci. Lett.* **67**, 151–161.

Clayton R. N. and Mayeda T. K. (1999) Oxygen isotope studies of carbonaceous chondrites. *Geochim. Cosmochim. Acta* **63**, 2089–2104.

Clayton R. N., Grossman L. and Mayeda T. K. (1973) A component of primitive nuclear composition in carbonaceous meteorites. *Science* **182**, 485–488.

Clayton R. N., Mayeda T. K., Goswami J. N. and Olsen E. J. (1991) The oxygen isotope record of Murchison and other carbonaceous chondrites. *Geochim. Cosmochim. Acta* **55**, 2317–2337.

Davis A. M., Hashizume K., Chaussidon M., Ireland T. R., Prieto C. A. and Lambert D. L. (2008) Oxygen in the Sun. In *Oxygen in the Solar System*, (Reviews in Mineralogy and Geochemistry, vol. 68), Mineralogical Society of America, pp. 73–92.

DeHart J. M., Lofgren G. E., Lu J., Benoit P. H. and Sears D. W. G. (1992) Chemical and physical studies of chondrites. 10. Cathodoluminescence and phase-composition studies of metamorphism and nebula processes in chondrules of type-3 ordinary chondrites. *Geochim. Cosmochim. Acta* **56**, 3791–3807.

Dodd R. T., Van Schmus W. RT. and Koffman D. M. (1967) A survey of the unequilibrated ordinary chondrites. *Geochim. Cosmochim. Acta* **31**, 921–951.

Gounelle M. and Meibom A. (2007) The oxygen isotopic composition of the Sun as a test of the supernova origin of Al-26 and Ca-41. *Astrophys. J.* **664**(2), L123–L125.

Grossman J. N. and Brearley A. J. (2005) The onset of metamorphism in ordinary and carbonaceous chondrites. *Meteorit. Planet. Sci.* **40**(1), 87–122.

Grossman J. N., Alexander C. M. O. D., Wang J. and Brearley A. J. (2002) Zoned chondrules in Semarkona: evidence for high- and low-temperature processing. *Meteorit. Planet. Sci.* **37**, 49–73.

Hand E. (2008) The solar system's first breath. *Nature* **452**, 159.

Howard E. C. (1802) Experiments and observations on certain stony and metalline substances, which at various times are said to have fallen on Earth; also on various kinds of native iron. *Philos. Trans. Roy. Soc. Lond.* **92**, 168–212.

Huang S., Lu J., Prinz M. K., Weisberg M. K., Benoit P. H. and Sears D. W. G. (1996) Chondrules: their diversity and role of open system processes during their formation. *Icarus* **122**, 316–346.

Huss G. R., Keil K. and Taylor G. J. (1981) The matrices of unequilibrated ordinary chondrites: implications for the origin and history of chondrites. *Geochim. Cosmochim. Acta* **45**, 33–51.

Hutchison R., Alexander C. M. O. and Barber D. J. (1987) The Semarkona meteorite: first recorded occurrence of smectite in an ordinary chondrite, and its implications. *Geochim. Cosmochim. Acta* **51**, 1875–1882.

Jones R. H. (1994) Petrology of FeO-poor, porphyritic pyroxene chondrules in the Semarkona chondrite. *Geochim. Cosmochim. Acta* **58**, 5325–5340.

Jones R. H., Saxton J. M., Lyon I. C. and Turner G. (2000) Oxygen isotopes in chondrule olivine and isolated olivine grains from the CO_3 chondrite Allan Hills A77307. *Meteorit. Planet. Sci.* **35**(4), 849–857.

Jones R. H., Leshin L. A., Guan Y. B., Sharp Z. D., Durakiewicz T. and Schilk A. J. (2004) Oxygen isotope heterogeneity in chondrules from the Mokoia CV3 carbonaceous chondrite. *Geochim. Cosmochim. Acta* **68**(16), 3423–3438.

Kimura Y., Nuth J. A., Chakpaborty S. and Thiemens M. H. (2007) Non-mass-dependent oxygen isotopic fractionation in smokes produced in an electrical discharge. *Meteorit. Planet. Sci.* **42**(7–8), 1429–1439.

Kita N. T., Nagahara H., Tachibana S., Fournelle J. H. and Valley J. W. (2007) Oxygen isotopic compositions of chondrule glasses in Semarkona (LL3.0): search for ^{16}O depleted components in chondrules. *Lunar and Planetary Science XXXVIII*, 1791.pdf.

Kobayashi S., Imai H. and Yurimoto H. (2003) New extreme O-16-rich reservoir in the early solar system. *Geochem. J.* **37**(6), 663–669.

Krot A. N., Yurimoto H., McKeegan K. D., Leshin L., Chaussidon M., Libourel G., Yoshitake M., Huss G. R., Guan Y. B. and Zanda B. (2006) Oxygen isotopic compositions of chondrules: Implications for evolution of oxygen isotopic reservoirs in the inner solar nebula. *Chem. Erde – Geochem.* **66**(4), 249–276.

Lauretta D. S. and McSween, Jr., H. Y. (2006) *Meteorites and the Early Solar System II*. University of Arizona Press, Tucson.

Lewis R. D., Lofgren G. E., Franzen H. F. and Windom K. E. (1993) The effect of Na vapour on the Na content of chondrules. *Meteorit. Planet. Sci.* **28**, 622–628.

Libourel G., Chaussidon M. and Krot A. N. (2008) Constraints on the origin of magnesian chondrules and on the gaseous reservoirs in the early solar system. *Lunar and Planetary Science Conference XXXIX*. #2017.

Lunine J., Graps A., O'Brien D. P., Morbidelli A., Leshin L. and Coradini A. (2007) Asteroidal sources of water based on dynamical simulations. *Lunar and Planetary Science Conference XXXVIII*. #1616.

Lyon I. C., Saxton J. M., Sears D. W. G., Symes S. and Turner G. (1999) Possible mass-independent oxygen-isotopic fractionation in the mesostasis of a Semarkona group A1 chondrule. *Meteorit. Planet. Sci.* **34**, A76–A77.

Lyons J. R. and Young E. D. (2005) CO self-shielding as the origin of oxygen isotope anomalies in the early solar nebula. *Nature* **435**(7040), 317–320.

Lyons J. R., Boney E. and Marcus R. A. (2008) Self-shielding at the X-point in the CO E(1)–X(0) band of CO. *Lunar and Planetary Science Conference*. #2265.

MacPherson G. J., Wark D. A. and Armstrong J. T. (1988) Primitive material surviving in chondrites: refractory inclusions. In *Meteorites and the Early Solar System* (eds. J. F. Kerridge and M. S. Matthews). University of Arizona Press, pp. 746–807.

Marcus R. A. (2004) Mass-independent isotope effect in the earliest processed solids in the solar system: a possible chemical mechanism. *J. Chem. Phys.* **121**(17), 8201–8211.

Matsunami S., Ninagawa K., Nishimura S., Kubona N., Yamamoto I., Kohata M., Wada T., Yamashita Y., Lu J., Sears D. W. G. and Nishimura H. (1993) Thermoluminescence and compositional zoning in the mesostasis of a Semarkona group A1 chondrule and new insights into the chondrule forming process. *Geochim. Cosmochim. Acta* **57**, 2101–2110.

McKeegan K.D., Jarzebinski G.J., Kallio, A.P., Mao P. H., Coath C. D., Kunihiro T., Wiens R.C., Alton J.H., Callaway M., Rodriguez M.C. and Burnett D. S. (2008) A first look at oxygen in a genesis concentrator sample. *Lunar and Planetary Science Conference*. #2020.

Merrill G. P. (1920) On chondrules and chondritic structure in meteorites. *Proc. Natl. Acad. Sci.* **6**, 449–472.

Nittler L. R. (2003) Presolar stardust in meteorites: recent advances and scientific frontiers. *Earth Planet. Sci. Lett.* **209**, 259–273.

Rai V. K. and Thiemens M. H. (2007) Mass independently fractionated sulfur components in chondrites. *Geochim. Cosmochim. Acta* **71**(5), 1341–1354.

Romero A. B. and Thiemens M. H. (2003) Mass-independent sulfur isotopic compositions in present-day sulfate aerosols. *J. Geophys. Res. – Atmos.* **108**(D16).

Sakamoto N., Seto Y., Itoh S., Kuramoto K., Fujino K., Nagashima K., Krot A. N. and Yurimoto H. (2007) Remnants of the early solar system water enriched in heavy oxygen isotopes. *Science* **317**(5835), 231–233.

Savarino J., Romero A., Cole-Dai J., Bekki S. and Thiemens M. H. (2003) UV induced mass-independent sulfur isotope fractionation in stratospheric volcanic sulfate. *Geophys. Res. Lett.* **30**(21).

Saxton J. M., Lyon I. C. and Turner G. (1995) Oxygen isotopes in forsterite grains from Julesburg and Allende – oxygen-16-rich material in an ordinary chondrite. *Meteoritics* **30**(5), 571–572.

Saxton J. M., Lyon I. C., Chatzitheodoridis E., Perera I. K., vanLierde P., Freedman P. and Turner G. (1996) The Manchester Isolab 54 ion microprobe. *Int. J. Mass Spectrom. Ion Process.* **154**(1–2), 99–131.

Saxton J. M., Lyon I. C. and Turner G. (1998) Oxygen isotopes in forsterite grains from Julesburg and Allende: oxygen-16-rich material in an ordinary chondrite. *Meteorit. Planet. Sci.* **33**(5), 1017–1027.

Scott E. R. D. (2007) Chondrites and the protoplanetary disk. *Annu. Rev. Earth Planet. Sci.* **35**, 577–620.

Scott E. R. D. and Taylor, G. J. (1983) Chondrules and other components in C, O, and E chondrites: similarities in the properties and origins. In *Proc. 14th Lunar Planet. Sci. Conf. J. Geophys. Res.*, vol. 88. pp. B275–B286.

Sears D. W. G. (2004) *The Origin of Chondrules and Chondrites*. Cambridge University Press.

Sears D. W. G., Grossman J. N., Melcher C. L., Ross L. M. and Mills A. A. (1980) Measuring the metamorphic history of unequilibrated ordinary chondrites. *Nature* **287**, 791–795.

Sears D. W. G., Huang S. and Benoit P. H. (1996) Open-system behaviour during chondrule formation. In *Chondrules and the Protoplanetary Disc* (eds. R. H. Hewins, R. H. Jones and E. R. D. Scott). University of Cambridge Press, pp. 221–232.

Sears D. W. G., Lu J., Benoit P. H., DeHart J. M. and Lofgren G. E. (1992) A compositional classification scheme for meteoritic chondrules. *Nature* **357**, 207–211.

Sears D. W. G., Lyon I., Saxton J. and Turner G. (1998) The oxygen isotopic properties of olivines in the Semarkona ordinary chondrite. *Meteorit. Planet. Sci.* **33**(5), 1029–1032.

Sears D. W. G., Lyon I. C., Saxton J. M., Symes S. and Turner G. (1999) Oxygen isotope heterogeneity in the mesostasis of a Semarkona group A1 chondrule. *Lunar and Planetary Science Conference XXX*, CD-ROM. #1406.

Sorby H. C. (1864) On the microscopical structure of meteorites. *Philos. Mag.* **28**, 157–159.

Thiemens M. H. (1996) Mass-independent isotopic effects in chondrites: the role of chemical processes. In *Chondrules and the Protoplanetary Disc* (eds. R. H. Hewins, R. H. Jones and E. R. D. Scott). University of Cambridge Press, pp. 107–118.

Thiemens M. H. (1999) Mass-independent isotope effects in planetary atmospheres and the early solar system. *Science* **283**, 341–345.

Thiemens M. H. (2006) History and applications of mass-independent isotope effects. *Annu. Rev. Earth Planet. Sci.* **34**, 217–262.

Thiemens M. H. and Heidenreich J. E. (1983) The mass-independent fractionation of oxygen – a novel isotope effect and its possible cosmochemical implications. *Science* **219**(4588), 1073–1075.

Young E. D. (2007) Time-dependent oxygen isotopic effects of CO self shielding across the solar protoplanetary disk. *Earth Planet. Sci. Lett.* **262**(3–4), 468–483.

Young E. D. and Russell S. S. (1998) Oxygen reservoirs in the early solar nebula inferred from an Allende CAI. *Science* **282**, 452–455.

Young E. D. and Lyons J. R. (2003) CO self shielding in the outer solar nebula: an astrochemical explanation for the oxygen isotope slope-1 line. **34** #1923.

Young E. D., Nagahara H., Mysen B. O. and Audet D. M. (1998) Non-Rayleigh oxygen isotope fractionation by mineral evaporation: theory and experiments in the system SiO_2. *Geochim. Cosmochim. Acta* **62**(18), 3109–3116.

Young E. D., Ash R. D., Galy A. and Belshaw N. S. (2002) Mg isotope heterogeneity in the Allende meteorite measured by UV laser ablation-MC-ICPMS and comparisons with O isotopes. *Geochim. Cosmochim. Acta* **66**(4), 683–698.

Young E. D., Kuramoto K., Marcus R. A., Yurimoto H. and Jacobsen S. B. (2008) Mass-independent oxygen isotope variation in the solar nebula. In *Oxygen in the Solar System*, (Reviews in Mineralogy and Geochemistry, vol. 68), Mineralogical Society of America, pp. 187–218.

Yurimoto H., Krot A. N., Choi B. G., Aleon J., Kunihiro T. and Brearley A. J. (2008) Oxygen isotopes of chondritic components. In *Oxygen in the Solar System*, vol. 68. pp. 141–186.

Yurimoto H. and Kuramoto K. (2004) Molecular cloud origin for the oxygen isotope heterogeneity in the solar system. *Science* **305**(5691), 1763–1766.

Zanda B., Hewins R. H., Bourot-Denise M., Bland P. A. and Albarede F. (2006) Formation of solar nebula reservoirs by mixing chondritic components. *Earth Planet. Sci. Lett.* **248**(3–4), 650–660.

Associate editor: Sara S. Russell